Parity oscillations and photon correlation functions in the Z_2-U(1) Dicke model at a finite number of atoms or qubits

Yu Yi-Xiang,[1,2,3] Jinwu Ye,[1,2,4] and CunLin Zhang[1]

[1]*Key Laboratory of Terahertz Optoelectronics, Ministry of Education, and Beijing Advanced Innovation Center for Imaging Technology, Department of Physics, Capital Normal University, Beijing 100048, China*

[2]*Department of Physics and Astronomy, Mississippi State University, P.O. Box 5167, Mississippi State, Mississippi 39762, USA*

[3]*School of Instrument Science and Opto-electronics Engineering, Institute of Optics and Electronics, BeiHang University, Beijing 100191, China*

[4]*Kavli Institute of Theoretical Physics, University of California, Santa Barbara, Santa Barbara, California 93106, USA*

(Received 29 December 2015; published 17 August 2016)

Four standard quantum optics models, that is, the Rabi, Dicke, Jaynes-Cummings, and Tavis-Cummings models, were proposed by physicists many decades ago. Despite their relative simple forms and many previous theoretical works, their physics at a finite N, especially inside the superradiant regime, remain unknown. In this work, by using the strong-coupling expansion and exact diagonalization (ED), we study the Z_2-U(1) Dicke model with independent rotating-wave coupling g and counterrotating-wave coupling g' at a finite N. This model includes the four standard quantum optics models as its various special limits. We show that in the superradiant phase, the system's energy levels are grouped into doublets with even and odd parity. Any anisotropy $\beta = g'/g \neq 1$ leads to the oscillation of parities in both the ground and excited doublets as the atom-photon coupling strength increases. The oscillations will be pushed to the infinite coupling strength in the isotropic Z_2 limit $\beta = 1$. We find nearly perfect agreement between the strong-coupling expansion and the ED in the superradiant regime when β is not too small. We also compute the photon correlation functions, squeezing spectrum, and number correlation functions that can be measured by various standard optical techniques.

DOI: 10.1103/PhysRevA.94.023830

I. INTRODUCTION

There are several well-known quantum optics models to study atom-photon interactions [1,2]. In the Rabi model [3], a single-photon mode interacts with a two-level atom with equal rotating-wave (RW) and counterrotating-wave (CRW) strengths. When the coupling strength is well below the transition frequency, the CRW term is effectively much smaller than the RW term, so it was dropped in the Jaynes-Cummings (JC) model [4]. The Rabi and JC models were extended, respectively, to the Dicke model [5] and the Tavis-Cummings (TC) model [6] with an assembly of N two-level atoms. Despite their relatively simple forms and many previous theoretical works [7–12], their solutions at a finite N, especially inside the superradiant regime, remain unknown. Here we address this outstanding problem. It is convenient to classify the four well-known quantum optics models in terms of simple symmetry: the TC and Dicke models as the U(1) and Z_2 Dicke models [13–15], respectively, and the JC and Rabi models are just $N = 1$ versions of the two.

Due to recent tremendous advances in technologies, ultrastrong couplings in cavity QED systems were achieved in at least two experimental systems: (i) Bose-Einstein condensate atoms inside an ultrahigh-finesse optical cavity [16–20] and (ii) superconducting qubits inside a microwave circuit cavity [21–24] or quantum dots inside a semiconductor microcavity [25]. In general, in such an ultrastrong-coupling regime, the system is described well by Eq. (1), dubbed the U(1)-Z_2 Dicke model [14,26,27], which includes the four standard quantum optics models as its various special limits. Despite many previous theoretical works on various special limits [7–12], their solutions at a finite N, especially inside the superradiant regime, remain unknown. Here we address this outstanding problem. Specifically, we study the U(1)-Z_2 Dicke model (1) at any finite N and any ratio $0 \leqslant g'/g = \beta \leqslant 1$ between the RW term g and the CRW term g' by strong-coupling expansion [28] and exact diagonalization (ED) [9,14,29]. We show that in the superradiant phase, the system's energy levels are grouped into doublets with even and odd parities, respectively. Any anisotropy $\beta \neq 1$ leads to the oscillation of parities in the ground and excited doublet states in the superradiant phase as g increases. In the Z_2 limit $\beta = 1$, all the oscillations are pushed to $g = \infty$. We find nearly perfect agreement between the strong-coupling expansion and the ED in the superradiant regime when β is not too small. We compute the photon correlation functions, squeezing spectrum, and number correlation functions that can be detected by the fluorescence spectrum, phase-sensitive homodyne detection, and a Hanbury-Brown-Twiss (HBT) type of experiment, respectively [1,2,30]. Experimental realizations are discussed and perspectives are outlined.

II. STRONG-COUPLING EXPANSION

In the strong-coupling limit, it is more convenient to start from the Z_2 limit with $\beta = 1$ and then treat $1 - \beta$ as a small parameter. One can rewrite the U(1)-Z_2 Dicke model [14] in its dual Z_2-U(1) presentation

$$H_{Z_2\text{-U(1)}} = \omega_a a^\dagger a + \omega_b J_z + \frac{g(1+\beta)}{\sqrt{N}}(a^\dagger + a)J_x - \frac{g(1-\beta)}{\sqrt{N}}(a^\dagger - a)iJ_y, \quad (1)$$

where ω_a and ω_b are the cavity photon frequency and the energy difference of the two atomic levels, respectively, and

g and $g' = \beta g$ $(0 \leqslant \beta \leqslant 1)$ are the atom-photon RW and CRW coupling, respectively. If $\beta = 0$, Eq. (1) reduces to the U(1) Dicke model [13–15] with the U(1) symmetry $a \to ae^{i\theta}$ and $\sigma^- \to \sigma^- e^{i\theta}$ leading to the conserved quantity $P = a^\dagger a + J_z$. The CRW g' term breaks the U(1) to Z_2 symmetry $a \to -a$ and $\sigma^- \to -\sigma^-$ with the conserved-parity operator $\Pi = e^{i\pi(a^\dagger a + J_z)}$. If $\beta = 1$, it becomes the Z_2 Dicke model [9,10,31].

After performing a rotation around the J_y axis by $\pi/2$, one can write $H = H_0 + V$, where $H_0 = \omega_a[a^\dagger a + G(a^\dagger + a)J_z]$, $G = \frac{g(1+\beta)}{\omega_a\sqrt{N}}$, and the perturbation $V = -\frac{\omega_b}{2}\{J_+[1 + \lambda(a^\dagger - a)] + J_-[1 - \lambda(a^\dagger - a)]\}$, where $\lambda = \frac{g(1-\beta)}{\omega_b\sqrt{N}}$ is a dimensionless parameter of order 1 when $1 - \beta$ is small in the large-g limit. In principle, the strong-coupling expansion is performed in the large-g limit $G \gg 1$, but with a small $1 - \beta$ such that λ is of order 1. In practice, as compared to ED, the method works well also when g is not too close to $g_c = \frac{\sqrt{\omega_a\omega_b}}{1+\beta}$ and β is not too close to the U(1) limit $\beta = 0$.

If we define $A = a + GJ_z$, then $H_0 = \omega_a[A^\dagger A - (GJ_z)^2]$ [29]. Because $[A, J_z] = 0$, we denote the simultaneous eigenstates of A and J_z as $|l\rangle_m|jm\rangle$, $m = -j, \ldots, j$ and $l = 0, 1, \ldots$. The eigenstates satisfy $J_z|jm\rangle = m\hbar|jm\rangle$ and $A_m^\dagger A_m|l\rangle_m = l|l\rangle_m$, where $A_m = a + Gm$ and $|l\rangle_m = D^\dagger(g_m)|l\rangle = D(-g_m)|l\rangle$, where $D(\alpha) = e^{\alpha a - \alpha^* a^\dagger}$, $g_m = mG$,

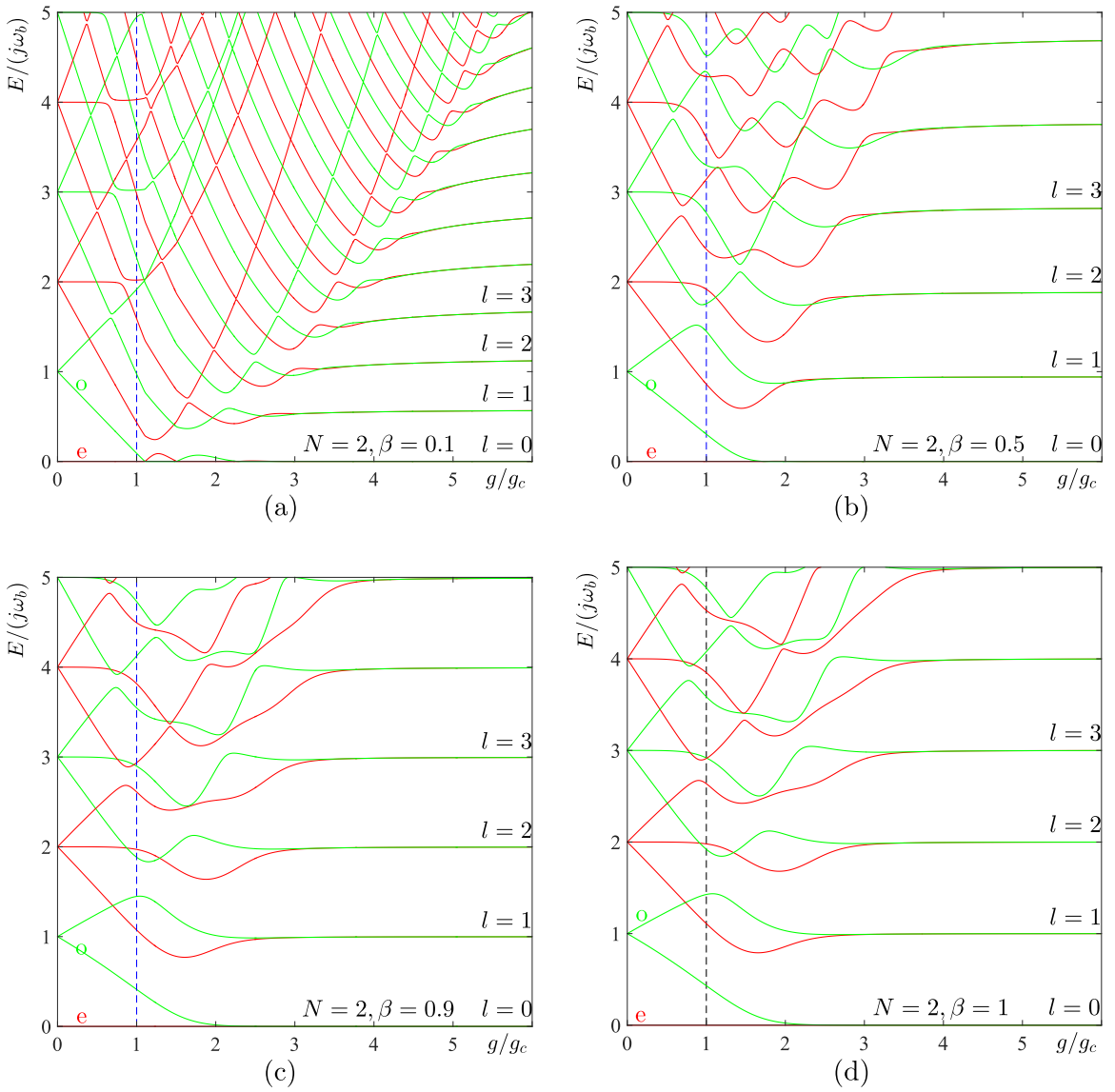

FIG. 1. The ED results for the energy levels at $N = 2$ and (a) $\beta = 0.1$, (b) $\beta = 0.5$, (c) $\beta = 0.9$, and (d) the Z_2 limit $\beta = 1$. For simplicity, we only show the $\omega_a = \omega_b$ case. The parity even in red and odd in green are indicated. We only label the atomic modes $l = 0,1,2,3, \ldots$. There are no, one-, and two-level crossing(s) in the normal regime at $l = 0,1,2$, respectively. When expanding the doublets at $l = 0,1, \ldots$, as g/g_c increases, there are infinite energy level crossings leading to the oscillations of parities at the ground states at $l = 0,1, \ldots$ manifolds shown in Fig. 3. As $\beta \to 1^-$, all the zeros are pushed to infinity in (d). There are no level crossings anymore between the even and odd parity pairs. Only the atomic energies at $l = 0,1,2, \ldots$ are labeled. As $g/g_c \to \infty$, they approach to $l\omega_a$ from below. This behavior was revealed by the strong-coupling expansion in the text. Note that the energy levels here are not directly experimentally detectable, but the photon correlations functions in Eqs. (10) and (11) are.

and $|l\rangle$ is just the l-photon Fock state. In particular, the ground state $|0\rangle_m = D(-g_m)|0\rangle$ is a photon coherent state. The zeroth-order eigenenergies are $H_0|l\rangle_m|jm\rangle = E^0_{l,m}|jm\rangle$ and $E^0_{l,m} = \omega_a(l - g_m^2)$. Using the parity operator $\Pi = e^{i\pi(a^\dagger a - J_x)}$, one can show that $\Pi|l\rangle_m|jm\rangle = (-1)^l|l\rangle_{-m}|j,-m\rangle$. Because the parity is a conserved quantity at any finite N, one can group all the eigenstates into even or odd under the parity operator $\Pi = e^{i\pi(a^\dagger a - J_x)}$:

$$|e\rangle = \frac{1}{\sqrt{2}}[|l\rangle_m|j,m\rangle + (-1)^l|l\rangle_{-m}|j,-m\rangle],$$
$$|o\rangle = \frac{1}{\sqrt{2}}[|l\rangle_m|j,m\rangle - (-1)^l|l\rangle_{-m}|j,-m\rangle]. \quad (2)$$

The ground state is a doublet at $|l=0\rangle_{\pm j}|j,\pm j\rangle$. In the large-$g$ limit, the excited states can be grouped into two sectors: (i) the atomic sector with the eigenstates $|l>0\rangle_{\pm j}|j,\pm j\rangle$ with the energies $l\omega_a$, where the first excited state $l=1$ with the energy ω_a is the remanent of the pseudo-Goldstone mode in the U(1) regime [14], and (ii) the optical sector with the eigenstates $|l\rangle_m|j,m\rangle$, $|m|<j$. The first excited state has the energy $\omega_o = E^0_{l,m=j-1} - E^0_{l,m=j} = \omega_a G^2(2j-1) = \frac{g^2(1+\beta)^2}{\omega_a}(\frac{2j-1}{2j})$ and is the remanent of the Higgs mode in the U(1) regime [14]. So in the strong-coupling limit there is wide separation between the atomic sector and the optical sector. This makes the strong-coupling expansion very effective in the exploration of physical phenomena in the superradiant regime.

III. GROUND-STATE ($l=0$) SPLITTING

The two degenerate ground state are $|1\rangle = |l=0\rangle_{-j}|j,-j\rangle$ and $|2\rangle = |l=0\rangle_j|j,j\rangle$ with the zeroth-order energy $E_0 = -\omega_a(Gj)^2$. Then we can determine the matrix elements in the 2×2 matrix, which is the effective Hamiltonian projected onto the two-dimensional subspace. By a second-order perturbation, one finds a nonzero diagonal matrix element

$$V_{11} = V_{22} = V_0(\lambda) = -\frac{\omega_b^2}{\omega_a}\frac{2j}{2j-1}\frac{1+\lambda^2}{G^2} < 0. \quad (3)$$

However, one needs to perform an $(N=2j)$-order perturbation (see Appendix A) to find the first nonzero contribution to the off-diagonal matrix element $V_{12} = V_{21} = \Delta_0(\lambda)$:

$$\Delta_0(\lambda) = -\frac{N^2\omega_b}{2}\left(\frac{\omega_b}{2\omega_a G^2}\right)^{N-1} e^{-(NG)^2/2} \times \sum_{l=0}^{N}\frac{\lambda^l}{(N-l)!}\sum_{n=0}^{[l/2]}\frac{(-1/2)^n(-NG)^{l-2n}}{n!(l-2n)!}, \quad (4)$$

where $[l/2]$ is the closest integer to $l/2$ and $\frac{\lambda}{G} = \frac{1-\beta}{1+\beta}\frac{\omega_a}{\omega_b}$. Setting $\lambda = 0$ in Eq. (4) leads to the splitting in the Z_2 Dicke model at $\beta = 1$ [Fig. 1(d)]:

$$\Delta_0 = -\frac{\omega_b}{(N-1)!}\left(\frac{\omega_b}{2\omega_a}\right)^{N-1}\frac{2g^2}{\omega_a^2}e^{-N(2/g^2\omega_a^2)} < 0, \quad (5)$$

which is always a negative quantity, and thus leads to even and odd parity as the ground state and the excited state in the $l=0$ and $m=j$ doublet in Eq. (2) having the energies $E_{o,e} = E_0 + V_0 \pm |\Delta_0|$ (Fig. 2).

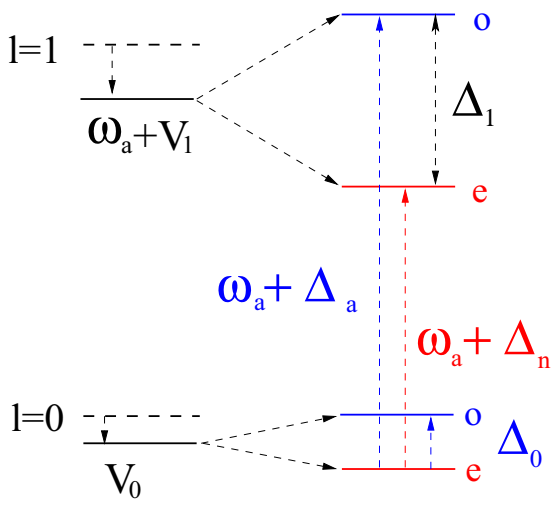

FIG. 2. Energy shifts $V_0 < 0$ and $V_1 < 0$ and splittings Δ_0 and Δ_1 of the ground state $l=0$ and the first excited state $l=1$. Shown here is the $\Delta_0 < 0$ and $\Delta_1 > 0$ case where the even parity state is the ground state at $l=0,1$. The blue and red dashed transition lines can be mapped out by photon and photon-number correlation functions (10) and (11), respectively.

Now we study the dramatic effects of the anisotropy $\lambda > 0$ encoded in Eq. (4). If removing the exponential factor $e^{-(G')^2/2}$, where $G' = NG$, Eq. (4) is a $2N$th polynomial of g. We find that it always has N positive zeros in g beyond the g_c (namely, fall into the superradiant regime). Perturbations higher than the Nth order will lead to other zeros at larger g, shown in Fig. 3(b). Any changing of sign in $\Delta_0(\lambda)$ leads to the exchange of parity in the ground state $l=0$ and $m=j$ in Eq. (20) [namely, Eq. (B1)] with the energies $E_{o,e} = E_0 + V_0(\lambda) \pm |\Delta_0(\lambda)|$ in Fig. 2. So any $\lambda > 0$ will lead to an infinite number of level crossings with alternative parities in the ground state, which is indeed observed in the ED results in Fig. 1 for the energy levels at $N=2$ and $\beta = 0.1, 0.5, 0.9$. It is the anisotropy that leads to the parity oscillations in the superradiant regime. However, at $\beta = 1$, the infinite level crossings are pushed to infinity, so there are no parity oscillations in Fig. 1(d) anymore [31].

IV. DOUBLET SPLITTING AT EXCITED STATES $l > 0$

Now we look at the energy splitting at $l > 0$. The diagonal matric element at $l=0$ in Eq. (3) can be easily generalized to the $l > 0$ case:

$$V_{11} = V_{22} = V_l(\lambda) = -\frac{\omega_b^2}{\omega_a}\frac{2j}{2j-1}\frac{1+\lambda^2(2l+1)}{G^2} < 0. \quad (6)$$

By performing an $(N=2j)$th-order perturbation, we also find a general (but a little bit complicated) expression for the off-diagonal matrix element $V_{12} = V_{21} = \Delta_l(\lambda)$. However, in the $G \gg 1$ limit, it can be simplified to

$$\Delta_l(\lambda) \sim \frac{(-1)^l}{l!}(G'^2)^l\Delta_0(\lambda), \quad (7)$$

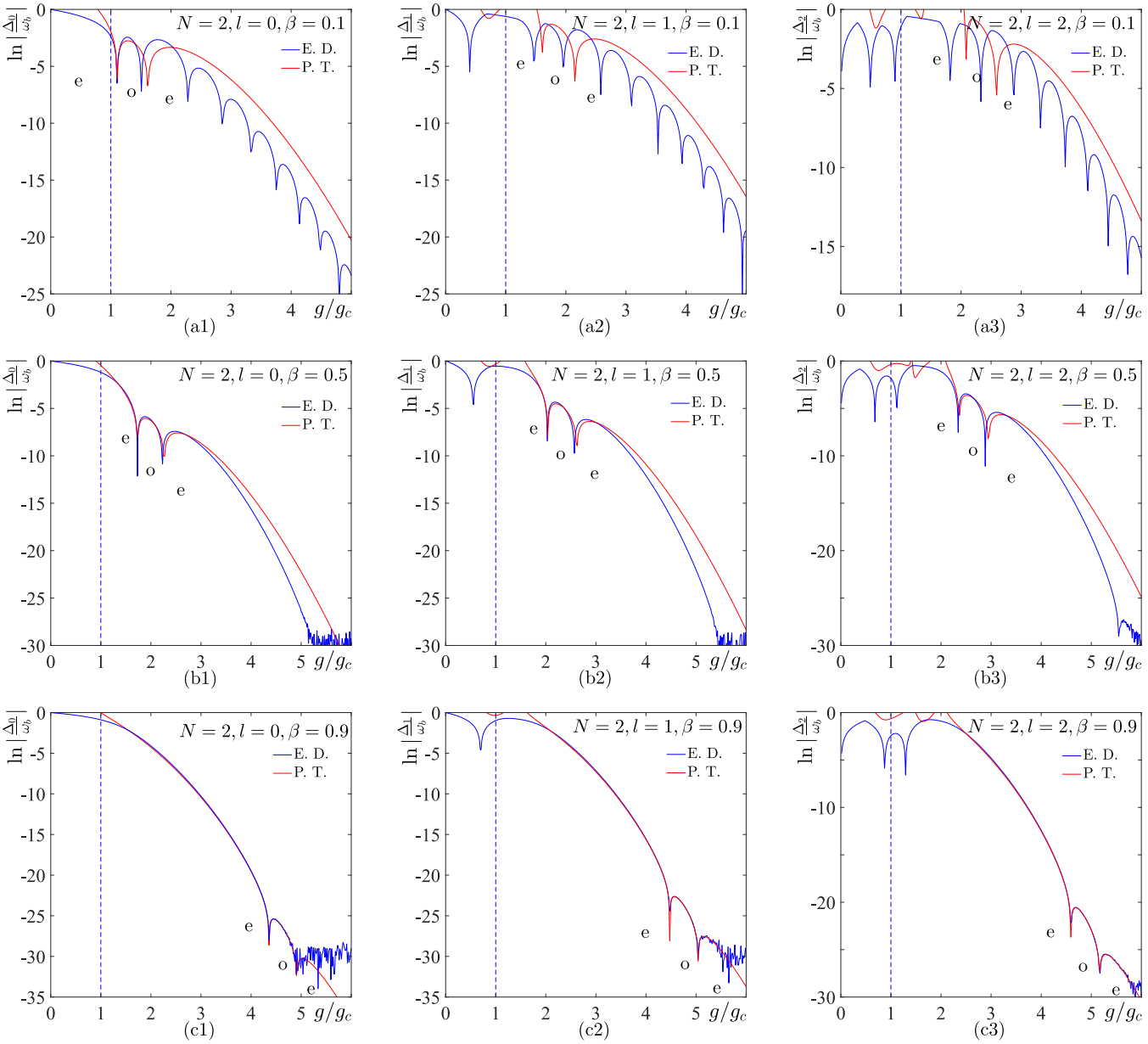

FIG. 3. Even-odd splitting Δ_l for $N = 2$ at (a) $\beta = 0.1$ and $l = 0$, (b) $\beta = 0.5$ and $l = 1$, and (c) $\beta = 0.9$ and $l = 2$ on a logarithmic scale $\ln|\frac{\Delta_l}{\omega_b}|$ versus g/g_c. The labels e and o are the parity of the ground states. Since $\Delta_0 > 0$, the ground state between the first two zeros in (a)–(c) has odd parity. The red and blue lines are from the strong-coupling expansion and the ED, respectively. The numerical sharp dips mean the zero splittings. They always start with even parity with oscillating parities at $l = 0,1,2$. There are also no, one-, and two-level crossings in the normal regime at $l = 0,1,2$. The ED gives an infinite number of zeros after the first $N = 2$ zeros, which can only be achieved from higher-order perturbations in the strong-coupling expansion. In (a) at $\beta = 0.1$, the strong-coupling results match well with those from the ED at $l = 0$, but not too well at $l = 1,2$ in the first $N = 2$ zeros. Even so, they match well the envelope of the splitting at $l = 0,1,2$ (namely, the maximum splitting). In both (b) and (c) the strong-coupling results match very well with those from ED in the first $N = 2$ zeros. The other zeros are far apart from the first $N = 2$ zeros and beyond the scope of the figure. In (a) or (b), if one follows the ground state with odd parity, there are some slight shifts of zero to the right at $l = 0,1,2$. In (c) the shifts are very small, as dictated by Eq. (7) in the limit $G = \frac{g}{g_c}\frac{1}{\sqrt{N}} \gg 1$. At too strong couplings, the ED may become (noise) unreliable due to the cutoff introduced in the ED.

where $\Delta_0(\lambda)$ is given in Eq. (4). It is enhanced due to the large prefactor G'^{2l}. Note that it is this oscillating sign $(-1)^l$ that leads to the even or odd parity state with an extra $(-1)^l$ in Eq. 2 with $m = j$ [namely, Eq. (B2)]. The lth levels have the energies $E_{o,e} = E_l^0 + V_l(\lambda) \pm |\Delta_l(\lambda)|$ and $E_l^0 = \omega_a[l - (Gj)^2]$ with $l = 1$ shown in Fig. 2. The diagonal part of the excited energy is

$$\begin{aligned}&\left[E_l^0 + V_l(\lambda)\right] - \left[E_0^0 + V_0(\lambda)\right]\\ &= l\omega_a - (|V_l| - |V_0|)\\ &= l\omega_a - \frac{\omega_b^2}{\omega_a}\frac{2j}{2j-1}\frac{1+2\lambda^2}{G^2} < l\omega_a, \end{aligned} \tag{8}$$

which approaches $l\omega_a$ from below in the $G \gg 1$ limit. This is indeed confirmed by the ED in Fig. 1.

Equation (7) shows that at the Nth-order perturbation, the number of zeros remains N and the positions of the zeros are independent of l in the $G \gg 1$ limit. This observation is indeed confirmed in the following ED results in Fig. 3.

V. EXACT DIAGONALIZATION RESULTS

Due to the λ term in Eq. (1), it is no longer convenient to perform the ED in the coherent basis used in [29], so we did the ED in the original (Fock) basis [9]. In the Fock space, the complete basis is $|n\rangle|j,m\rangle$, $n = 0,1,2,\ldots,\infty$, $j = N/2$, and $m = -j,\ldots,j$, where n is the number of photons and $|j,m\rangle$ are the Dicke states. In performing the ED, following [9], one has to use a truncated basis $n = 0,1,\ldots,n_c$ in the photon sector where $n_c \sim 100$ is the maximum photon number in the artificially truncated Hilbert space. As long as the low-energy levels in Figs. 3 and 1 are well below $n_c\omega_a$, then the energy levels should be very close to the exact results without the truncation (namely, sending $n_c \to \infty$). However, the ED may not be precise anymore when g gets too close to the upper cutoff introduced in the ED calculations as shown in Fig. 3(c).

VI. COMPARISON BETWEEN THE STRONG-COUPLING EXPANSION AND ED

In Figs. 3(a)–3(c) we compare Eqs. (4) and (7) with the ED results on the energy-level splitting between the doublets with even and odd parity for $N = 2$ at $\beta = 0.1,0.5,0.9$ and $l = 0,1,2$. We find that the first N zeros (or parity oscillations) from the strong-coupling expansion match those from the ED nearly perfectly at $\beta = 0.5,0.9$ in the superradiant regime. Of course, the ED may not be precise anymore when g gets too close to the upper cutoff introduced in the ED calculation as shown in Fig. 3(d). In fact, the first $N = 2$ zeros of Eq. (4) can be found exactly as the two positive roots

$$G_{\mp} = \left(\sqrt{1+8\frac{1+\beta}{1-\beta}} \mp 1\right)\Big/4, \tag{9}$$

which fall in the superradiant regime. The spacing between the two roots $\Delta(\frac{g}{g_c}) = \frac{1}{\sqrt{2}}$ is independent of β as shown in Figs. 3(c) and 3(d). As $\beta \to 1^-$, both roots $\sim(1-\beta)^{-1/2}$ are pushed toward infinity.

Equation (7) is also confirmed by the ED shown in Fig. 3(d) for $N = 2$, $\beta = 0.9$, and $l = 0,1,2$ where the positions of the first $N = 2$ zeros only depend on l very weakly. So between the two zeros, at $l = 0,1,2,\ldots$, the energy levels are in the pattern $(e,o),(e,o),\ldots$ when $\Delta_0(\lambda) < 0$, as shown in Fig. 2 [or $(o,e),(o,e),\ldots$ when $\Delta_0(\lambda) > 0$].

VII. PHOTON, SQUEEZING, AND NUMBER CORRELATION FUNCTIONS

Note that the energy-level structures in Figs. 3(a)–3(c) are not directly experimentally measurable. So it is very important to evaluate various photon correlation functions graphically shown in Fig. 2, which can be directly measured through leaking cavity photons by various standard quantum optics detection methods. In order to calculate the photon correlation functions in the strong-coupling limit, one needs to find not only the energy levels as done in the previous sections and in Fig. 2, but also the wave functions given in Appendix B. Using the Lehmann representations, we find there is no first-order correction to the normal photon correlation function, but there is one $\sim 1/G^2$ to the anomalous photon correlation function:

$$\begin{aligned}\langle a(t)a^{\dagger}(0)\rangle &= Ae^{-i|\Delta_0|t} + e^{-i(\omega_a+\Delta_a)t},\\ \langle a(t)a(0)\rangle &= Ae^{-i|\Delta_0|t} - Be^{-i(\omega_a+\Delta_a)t},\end{aligned} \tag{10}$$

where $A = (Gj)^2 = N\frac{g^2(1+\beta)^2}{4\omega_a^2} \sim G^2$ is the photon number in the ground state [32] and $B = \frac{\lambda^2}{G^2}(\frac{\omega_b}{2\omega_a})^2\frac{2j}{2j-1} \sim 1/G^2$ and $\Delta_a = (V_1 - V_0) + \frac{1}{2}(|\Delta_1| + |\Delta_0|)$, as shown in Fig. 2. One can see that the anomalous spectral weight $-B \sim (\lambda/G)^2$ is negative and completely due to λ (away from the Z_2 limit). So the B term in the anomalous photon correlation function can reflect precisely the anisotropy β and can be easily detected in phase-sensitive homodyne measurements [30].

Similarly, we also find the first-order correction $\sim 1/G^2$ to the photon-number correlation function

$$\langle n(t)n(0)\rangle - \langle n\rangle^2 = A[1+B]^2e^{-i(\omega_a+\Delta_n)t}, \tag{11}$$

where $\Delta_n = (V_1 - V_0) - \frac{1}{2}(|\Delta_1| - |\Delta_0|)$, as shown in Fig. 2, and $\langle n\rangle = A$ is the photon number in the ground state that does not receive first-order correction. From Eqs. (10) and (11) one can see that Δ_0 can be directly extracted from the very first frequency in Eq. (10), while $|\Delta_1| = \Delta_a - \Delta_n$ and $V_1 - V_0 = (\Delta_a + \Delta_n)/2 - |\Delta_0|$. So all the parameters of the cavity systems such as the doublet splittings $\Delta_0(\lambda)$ and $\Delta_1(\lambda)$ and energy-level shifts $V_1 - V_0$ in Fig. 2 can be extracted from the photon normal and anomalous Green's functions (10) and photon-number correlation functions (11). Their spectral weights also contain detailed information about the wave functions of the system's energy levels. They can be measured by photoluminescence, phase-sensitive homodyne detection, and HBT-type experiments [30], respectively.

VIII. EXPERIMENTAL REALIZATIONS AND DETECTIONS

In order to observe the parity oscillation effects, one has to move away from the Z_2 limit realized in the experiments [18–20], namely, $0 < \beta < 1$. This has been realized in the recent experiment [27] with $N \sim 10^5$ cold atoms inside an optical cavity that can tune β from 0 to 1. In view of recent experimental advances to manipulate a few atoms inside an optical cavity [33,34], it should be practical to reduce the number of atoms to a few in the experiment [27]. In circuit QED systems, there are various experimental setups such as charge, flux, phase qubits, or qutrits and the couplings could be capacitive or inductive through Λ, V, Ξ, or the Δ shape [35]. In particular, continuously changing $0 < \beta < 1$ has been achieved in a recent experiment [24]. As shown in [14], the repulsive qubit-qubit interaction also reduces the critical coupling g_c.

From Fig. 3(a1), at $N = 2$, $\beta = 0.1$, and $l = 0$, one can estimate the maximum splitting between the first two zeros $\Delta_0 \sim 0.1\omega_a$, which is easily experimentally measurable. Here Δ_l increases as $l = 1,2$ as shown in Figs. 3(a2) and 3(a3). At $\beta = 0.5$ in Fig. 3(b1), Δ_0 decreases to $\sim 0.01\omega_a$, which is still easily measurable. The splittings at $\beta = 0.2,0.3,0.4$ falling in the range $0.01\omega_a < \Delta_0 < 0.1\omega_a$ are shown in Fig. 4. At $\beta = 0.9$ in Fig. 3(c1), Δ_0 decreases to $\sim 10^{-11}\omega_a$, which may become difficult to measure. However, in view of recent advances in the precision measurements in the detection of elusive gravitational waves [36], it is also possible to measure such a tiny splitting by phase-sensitive homodyne detection [20]. So the parity oscillations can be easily measured experimentally when β is not too close to the Z_2 limit with a finite number $N = 2$–9 of atoms or qubits inside a cavity. As stated in the preceding section, the photon normal and anomalous and photon-number correlation functions in Eqs. (10) and (11) can be measured by photoluminescence, phase-sensitive homodyne detection, and HBT-type experiments [30], respectively.

IX. CONCLUSION

Four standard quantum optics models at finite N were proposed by physicists many decades ago. Their importance in quantum and nonlinear optics ranks the same as the bosonic or fermionic Hubbard models and Heisenberg models in strongly correlated electron systems and the Ising models in statistical mechanics [37]. Despite their relatively simple forms and many previous theoretical works, their solutions at finite N, especially inside the superradiant regime, remain unknown. In this work we addressed this outstanding historical problem by using the strong-coupling expansion and ED. We were able to analytically calculate remarkably accurately various photon correlation functions in the superradiant regime except when β is too small, where nondegenerate or degenerate perturbations near the U(1) limit($\beta = 0$) work well [14]. The present work may inspire several new directions. From the wave functions given in Appendix B, it would be interesting to evaluate the effects of parity oscillations on atom-photon entanglements at a given $l = 0,1,2,\ldots$ manifold. It is important to incorporate the effects of the external pumping and cavity photon decays [30] to evaluate the photon correlations functions in Eqs. (10) and (11) using the Keldysh nonequilibrium Green's-function approach. It would be tempting to study the arrays of cavities leading to the Z_2-(1) Dicke lattice models [38] with general $0 < \beta < 1$.

ACKNOWLEDGMENTS

We acknowledge NSF Grant No. DMR-1161497 for support. The work at KITP was supported by NSF Grant No. PHY11-25915. The work of C.Z. was supported by National Keystone Basic Research Program (973 Program) under Grants No. 2007CB310408 and No. 2006CB302901.

APPENDIX A: DERIVATION OF EQ. (4)

In this Appendix we give the derivation of Eq. (4). In addition, we provide the wave functions up to the first order in $1/G^2$ in the strong-coupling expansion that are needed to evaluate various photon correlation functions. We also provide some additional ED results that complement those presented in the main text.

The first nonvanishing contribution to the off-diagonal matrix element is through $(N = 2j)$th-order perturbation $V_{12} = V_{21} = \Delta_0(\lambda) = \langle 2|H_N|1\rangle$, where $H_N = P_0 V \frac{1-P_0}{E_0-H_0} V \cdots \frac{1-P_0}{E_0-H_0} V P_0$, which contains N interactions V and $N-1$ propagators $\frac{1-P_0}{E_0-H_0}$, E_0 is the ground-state energy, and P_0 is the projection onto the ground-state manifold spanned by the doublets $|1\rangle$ and $|2\rangle$.

Using the eigenvalues $E^0_{l,m} = \omega_a(l - g_m^2)$ and $g_m = mG$ and inserting the eigenstates $|l\rangle_m|j,m\rangle$ of H_0 into the expression leading to

$$\Delta_0(\lambda) = -\left(\frac{\omega_b}{2\omega_a}\right)^{N-1} \frac{\omega_b}{2}\sqrt{N} \sum_{\{l\}} \prod_{m=-j+1}^{j-1} [A(l_{j+m+1},l_{j+m})] \frac{\sqrt{j(j+1)-m(m+1)}}{l_{j+m}+G^2(j^2-m^2)} \times [{}_{-j+1}\langle l_1|[|0\rangle_{-j} + \lambda|1\rangle_{-j}], \tag{A1}$$

where $A(l_{j+m+1},l_{j+m}) = {}_{m+1}\langle l_{j+m+1}|1+\lambda(a^\dagger - a)|l_{j+m}\rangle_m = {}_{m+1}\langle l_{j+m+1}|[|l_{j+m}\rangle_m + \lambda\sqrt{l_{j+m}+1}|l_{j+m}+1\rangle_m - \lambda\sqrt{l_{j+m}}|l_{j+m}-1\rangle_m]$, the product is over the $N-1$ intermediate states $|l\rangle_m|jm\rangle$, $m = -j+1,\ldots,j-1$, connecting $|1\rangle$ to $|2\rangle$ and $\{l\} = l_1,\ldots,l_{2j-1},l_{2j} = 0$.

In the $G \gg 1$ limit, it is justified to drop the l_{j+m} dependence in the denominator; thus Eq. (A1) simplifies to

$$\Delta_0(\lambda) = -\left(\frac{\omega_b}{2\omega_a G^2}\right)^{N-1} \frac{\omega_b}{2}\sqrt{N} \prod_{m=-j+1}^{j-1} \frac{\sqrt{j(j+1)-m(m+1)}}{j^2-m^2} {}_j\langle 0|[1+\lambda(a^\dagger - a)]^N|0\rangle_{-j}. \tag{A2}$$

The overlapping matrix element between the two ground states can be evaluated as

$${}_j\langle 0|[1+\lambda(a^\dagger - a)]^N|0\rangle_{-j} = \sum_{n=0}^{N} \lambda^n C_N^n E_n, \tag{A3}$$

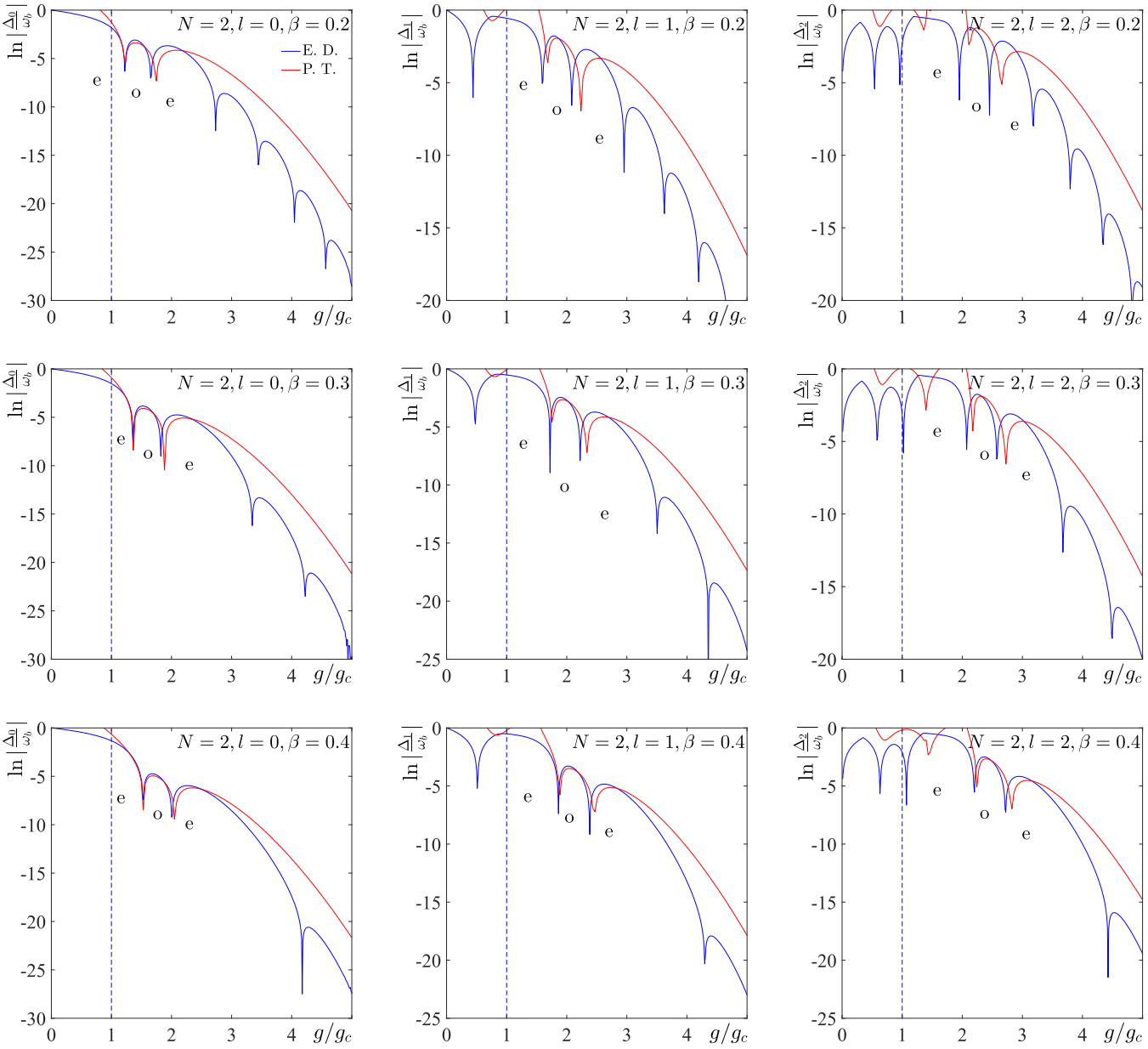

FIG. 4. Even-odd splitting Δ_l for $N=2$ at $\beta=0.2,0.3,0.4$ at $l=0,1,2$ on a logarithmic scale $\ln|\frac{\Delta_l}{\omega_b}|$ versus g/g_c. The notation is the same as in Fig. 3. The strong-coupling expansion works very well in the ground-state doublet $l=0$. There are some small deviations from the ED at the excited doublets $l=1,2$ when $\beta=0.2$, but the deviations decrease when $\beta=0.3,0.4$. As β increases, the other zeros start to gradually move away from the first two. As shown in the text, all the splittings are easily experimentally measurable.

where E_n means taking the coefficient of $x^n/n!$ in the Tylor expansion of $E(x)=e^{-(G'+x)^2/2}$, where $G'=NG$. Taking the coefficient leads to

$$
\begin{aligned}
&{}_j\langle 0|[1+\lambda(a^\dagger-a)]^N|0\rangle_{-j} \\
&\quad = e^{-(G')^2/2}\sum_{l=0}^{N}\frac{N!\lambda^l}{(N-l)!}\sum_{n=0}^{[l/2]}\frac{(-1/2)^n(-\lambda G')^{l-2n}}{n!(l-2n)!},
\end{aligned}
\tag{A4}
$$

where $[l/2]$ is the closest integer to $l/2$. Evaluating the product $\prod_{m=-j+1}^{j-1}\frac{\sqrt{j(j+1)-m(m+1)}}{j^2-m^2}=\frac{\sqrt{2j}}{(2j-1)!}$ in Eq. (A2) leads to Eq. (4).

APPENDIX B: WAVE FUNCTIONS BY STRONG-COUPLING EXPANSION

The zeroth-order ground states with even and odd parities of the system are at the $l=0$ and $m=j$ sector in Eq. (2):

$$
\begin{aligned}
|e\rangle_0 &= \frac{1}{\sqrt{2}}[|l=0\rangle_j|j,j\rangle+|l=0\rangle_{-j}|j,-j\rangle], \\
|o\rangle_0 &= \frac{1}{\sqrt{2}}[|l=0\rangle_j|j,j\rangle-|l=0\rangle_{-j}|j,-j\rangle],
\end{aligned}
\tag{B1}
$$

with the energies $E_{o,e}=E_0+V_0(\lambda)\pm|\Delta_0(\lambda)|$ shown in Fig. 2. Using straightforward nondegenerate perturbation

expansion, we find the first-order correction in $1/G^2$ to the even-odd ground states at $l=0$ in Eq. (B1):

$$|\alpha\rangle_1 = \frac{\omega_b}{2\omega_a}\sqrt{2j}\sum_l \frac{{}_{j-1}\langle l|1-\lambda(a^\dagger - a)|l=0\rangle_j}{l+G^2(2j-1)}\frac{1}{\sqrt{2}}[|l\rangle_{j-1}|j,j-1\rangle + \alpha(-1)^l|l\rangle_{-j+1}|j,-j+1\rangle]$$
$$+\left(\frac{\omega_b}{2\omega_a}\right)^2 2j\sum_{l,l'\neq 0}\frac{{}_j\langle l'|1+\lambda(a^\dagger - a)|l\rangle_{j-1}\cdot{}_{j-1}\langle l|1-\lambda(a^\dagger - a)|l=0\rangle_j}{l'[l+G^2(2j-1)]}\frac{1}{\sqrt{2}}[|l'\rangle_j|j,j\rangle + \alpha(-1)^{l'}|l'\rangle_{-j}|j,-j\rangle], \quad \text{(B2)}$$

where $\alpha=\pm$ for $\alpha=e,o$, respectively. Indeed, it shows that the even (odd) parity ground state is mixed with only other even (odd) parity states as dictated by the parity conservation of the Hamiltonian at any finite N. One can see that the first-order correction to the ground-state wave function consists of two parts: the first part (line) is in the high-energy optical sector and the second part (line) is in the low-energy atomic sector.

The zeroth-order lth level states with even and odd parities of the system are at $l,m=j$ in Eq. (2):

$$|e,l\rangle = \frac{1}{\sqrt{2}}[|l\rangle_j|j,j\rangle + (-1)^l|l\rangle_{-j}|j,-j\rangle],$$
$$|o,l\rangle = \frac{1}{\sqrt{2}}[|l\rangle_j|j,j\rangle - (-1)^l|l\rangle_{-j}|j,-j\rangle], \quad \text{(B3)}$$

with the energies $E_{o,e}=E_l^0+V_l(\lambda)\pm|\Delta_l(\lambda)|$ and $E_l^0=\omega_a[l-(Gj)^2]$ in Fig. 2. Similarly, one can find the first-order correction to the two doublets at $l=1$ in Eq. (B3) by making the following replacements in Eq. (B2): changing $|l=0\rangle_j$ to $|l=1\rangle_j$, the denominator $[l+G^2(2j-1)]$ to $[l-1+G^2(2j-1)]$, and the sum subscript $l'\neq 0$ to $l'\neq 1$. These wave functions are used to calculate the photon correlation functions (10) and (11).

APPENDIX C: ADDITIONAL EXACT DIAGONALIZATION RESULTS

In this Appendix we show the results on even-odd splitting Δ_l for $N=2$ at $\beta=0.2,0.3,0.4$ at $l=0,1,2$, shown in Fig. 4. They make up the results between $\beta=0.1$ and $\beta=0.5$ shown in Fig. 3. In particular, they describe how the maximum splitting between the first two zeros Δ_0 monotonically decreases from $\Delta_0\sim 0.1\omega_a$ at $\beta=0.1$ to $\Delta_0\sim 0.01\omega_a$ at $\beta=0.5$ and also how the other zeros separate from the first two as β increases.

We also made the comparisons between strong-coupling expansions and the ED on the doublet splittings for $N=5$ at $\beta=0.1,0.5,0.9,1$ and $l=0,1,2$ and found agreement similar to that at $N=2$, shown in Fig. 3.

[1] D. F. Walls and G. J. Milburn, *Quantum Optics* (Springer, Berlin, 1994).

[2] M. O. Scully and M. S. Zubairy, *Quantum Optics* (Cambridge University Press, Cambridge, 1997).

[3] I. I. Rabi, Phys. Rev. **49**, 324 (1936); **51**, 652 (1937).

[4] E. T. Jaynes and F. W. Cummings, Proc. IEEE **51**, 89 (1963).

[5] R. H. Dicke, Phys. Rev. **93**, 99 (1954).

[6] M. Tavis and F. W. Cummings, Phys. Rev. **170**, 379 (1968).

[7] K. Hepp and E. H. Lieb, Ann. Phys. (NY) **76**, 360 (1973); Y. K. Wang and F. T. Hioe, Phys. Rev. A **7**, 831 (1973).

[8] V. N. Popov and S. A. Fedotov, Sov. Phys. JETP **67**, 535 (1988); V. N. Popov and V. S. Yarunin, *Collective Effects in Quantum Statistics of Radiation and Matter* (Kluwer Academic, Dordrecht, 1988).

[9] C. Emary and T. Brandes, Phys. Rev. Lett. **90**, 044101 (2003); Phys. Rev. E **67**, 066203 (2003); N. Lambert, C. Emary, and T. Brandes, Phys. Rev. Lett. **92**, 073602 (2004).

[10] J. Vidal and S. Dusuel, Europhys. Lett. **74**, 817 (2006). For the Z_2 Dicke model $\beta=1$, the ground-state photon number at the quantum critical point (QCP) was found to scale as $\langle n_{ph}\rangle\sim cN^{1/3}$ [10], which is a direct consequence of finite-size scaling near a QCP with infinite coordination numbers [11]. For the general U(1)-Z_2 Dicke model (1) with $0<\beta<1$, the normal to the superradiant transitions at $N=\infty$ shares the same universality class as the Z_2 limit at $\beta=1$, so only the coefficient c depends on β. As shown in this paper, the dramatic qualitative differences and phenomena due to $\beta\neq 1$ show up only away from the QCP in the superradiant regime.

[11] R. Botet, R. Jullien, and P. Pfeuty, Phys. Rev. Lett. **49**, 478 (1982); Phys. Rev. B **28**, 3955 (1983).

[12] There is a "formal" exact solution on the Z_2 Dicke model at $N=1$ and $\beta=1$. D. Braak, Phys. Rev. Lett. **107**, 100401 (2011). Unfortunately, this exact solution is essentially useless in any practical computations. It is also difficult to extract any physics from it. For example, it is difficult to even derive $\langle n_{ph}\rangle\sim N^{1/3}$ scaling near the QCP [10] and also any phenomenon achieved in the present paper in the superradiant regime from the formally exact solution even at the simplest case $N=1$ and $\beta=1$. It would be impossible to calculate the dynamic photon correlation functions (10) and (11).

[13] J. Ye and C. Zhang, Phys. Rev. A **84**, 023840 (2011).

[14] Y. Yi-Xiang, J. Ye, and W. M. Liu, Sci. Rep. **3**, 3476 (2013).

[15] Y. Yi-Xiang, J. Ye, W. M. Liu, and C. Zhang, arXiv:1506.06382.

[16] F. Brennecke *et al.*, Nature (London) **450**, 268 (2007).

[17] Y. Colombe *et al.*, Nature (London) **450**, 272 (2007).

[18] A. T. Black, H. W. Chan, and V. Vuletic, Phys. Rev. Lett. **91**, 203001 (2003).

[19] K. Baumann *et al.*, Nature (London) **464**, 1301 (2010).

[20] K. Baumann, R. Mottl, F. Brennecke, and T. Esslinger, Phys. Rev. Lett. **107**, 140402 (2011).

[21] A. Wallraff *et al.*, Nature (London) **431**, 162 (2004).

[22] G. Gunter *et al.*, Nature (London) **458**, 178 (2009).

[23] A. A. Anappara, S. De Liberato, A. Tredicucci, C. Ciuti, G. Biasol, L. Sorba, and F. Beltram, Phys. Rev. B **79**, 201303(R) (2009).
[24] T. Niemczyk *et al.*, Nat. Phys. **6**, 772 (2010).
[25] J. P. Reithmaiser *et al.*, Nature (London) **432**, 197 (2004); T. Yoshie *et al.*, *ibid.* **432**, 200 (2004); K. Hennessy *et al.*, *ibid.* **445**, 896 (2007).
[26] F. Dimer, B. Estienne, A. S. Parkins, and H. J. Carmichael, Phys. Rev. A **75**, 013804 (2007)
[27] M. P. Baden, K. J. Arnold, A. L. Grimsmo, S. Parkins, and M. D. Barrett, Phys. Rev. Lett. **113**, 020408 (2014).
[28] For strong-coupling expansions and spin-wave expansion in spin-orbit coupled lattice systems, see F. Sun, J. Ye, and W.-M. Liu, Phys. Rev. A **92**, 043609 (2015); arXiv:1502.05338.
[29] Q.-H. Chen, Y.-Y. Zhang, T. Liu, and K.-L. Wang, Phys. Rev. A **78**, 051801(R) (2008).
[30] J. Ye, T. Shi, and L. Jiang, Phys. Rev. Lett. **103**, 177401 (2009); T. Shi, L. Jiang, and J. Ye, Phys. Rev. B **81**, 235402 (2010); J. Ye, F. Sun, Y.-X. Yu, and W. Liu, Ann. Phys. (NY) **329**, 51 (2013).
[31] It is tempting to try to sort out if there is an extra symmetry at the Z_2 limit $\beta = 1$. Taking Eq. (1), one can see the last two terms exchange under the transformation $a \to e^{i\pi/2}a$ and $\sigma_- \to e^{i\pi/2}\sigma_-$. It is also easy to see the Hamiltonian has the symmetry $\mathcal{T} \times R(y,\pi)$ or $\mathcal{T} \times R(x,\pi) \times Z_2^a$, where $\mathcal{T}$ is the time-reversal symmetry, $R(y,\pi)$ and $R(x,\pi)$ are the spin rotations by π around the y or x axis, respectively, and Z_2^a is $a \to -a$. So there is no extra symmetry at the Z_2 limit.
[32] In the first line in Eq. (10), setting $t = 0$ and using $[a,a^\dagger] = 1$, one can also see the photon number in the ground state $\langle n \rangle = A$.
[33] W. S. Bakr *et al.*, Science **329**, 547 (2010).
[34] F. Serwane *et al.*, Science **332**, 336 (2011).
[35] For reviews see J. Q. You and F. Nori, Nature (London) **474**, 589 (2011); S. M. Girvin, Circuit QED: superconducting qubits coupled to microwave photons, in *Quantum Machines: Measurement and Control of Engineered Quantum Systems*, edited by M. Devoret, B. Huard, R. Schoelkopf, and L. F. Cugliandolo, Les Houches, Session XCVI (Oxford University Press, Oxford, 2011), p. 22.
[36] B. P. Abbott *et al.* (LIGO Scientific Collaboration and Virgo Collaboration), Phys. Rev. Lett. **116**, 061102 (2016).
[37] A. Auerbach, *Interacting Electrons and Quantum Magnetism* (Springer Science & Business Media, New York, 1994).
[38] M. Schiró, M. Bordyuh, B. Öztop, and H. E. Tureci, Phys. Rev. Lett. **109**, 053601 (2012). For a review on experimental implementations, see A. A. Houck, H. E. Tureci, and J. Koch, Nat. Phys. **8**, 292 (2012).